

Trehalose-Induced Variation in Mechanical Properties of Vesicles in Aqueous Solution

Jaehyun Hur¹ · Jin-Won Park²

Received: 1 June 2015 / Accepted: 24 July 2015 / Published online: 2 August 2015
© Springer Science+Business Media New York 2015

Abstract The effect of the trehalose incorporation on the nanomechanical properties of dipalmitoylphosphatidylcholine vesicles was studied using atomic force microscope (AFM) on mica surface. The vesicles were prepared only with the variation in the trehalose concentration and adsorbed on the mica surface. After the morphology of the adsorbed vesicles was characterized, the behavior of an AFM tip into the vesicle was monitored using the plot of the tip displacement versus the tip deflection. It was observed that the breakthrough of the tip into the vesicles occurred two times. Each breakthrough represented each penetration of the tip into each layer. Force data prior to the first breakthrough fitted well with the Hertzian model to estimate Young's modulus and bending modulus of the vesicles. It was found that the Young's modulus and bending modulus decreased proportionally to the increase in the trehalose concentration up to 0.5 of trehalose to lipid. However, above 0.5, the moduli were a little varied with the increase. In the identical measurements at glucose, just a slight change in the moduli was observed with the increase in the glucose composition from 0 % glucose up to even 2:1 ratio of glucose:lipid. These results in the mechanical properties seem attributable to the osmotic and volumetric effects on the headgroup packing disruption.

Keywords Trehalose · Biological membranes · Young's modulus · Bending modulus

Introduction

Sugars have wide occurrence in living organisms (Crowe and Crowe 1992). Soluble sugars stabilize liposomes, intact membranes, and whole cells against desiccation and fusion caused by freezing or freeze-drying (Crowe et al. 1983, 1985; Leslie et al. 1994). Therefore, studies on the effects of saccharides on a cell membrane, such as on its permeability and stability, are very important for understanding its functions, such as protection and preservation (Crowe et al. 1983; Carpenter et al. 1987). For the studies, artificial membrane systems have been useful as simplified biomembranes (Fendler 1982). Especially, trehalose has been investigated as a disaccharide which indicates the most effective protection against water stress among saccharides (Lerbret et al. 2007). Furthermore, it has been found that trehalose induced the structure preservation against freezing or drying in the systems (Crowe and Crowe 1995). Consequently, it is proposed that trehalose avoided the transition between gel and liquid crystalline phase during rehydration and inhibited the leakage from the system inside due to packing defect (Lambruschini et al. 2000).

The mechanical properties of phospholipids present in membranes are of great interest because they play an important role in the aspects of vesicle-related processes and the interaction with antimicrobial compounds (Svetina and Zeks 1996). Atomic force microscope (AFM) has been widely used for measurements of forces of interaction between the AFM probe and the surface, giving information about the physical properties of sample surface (Fang et al. 2000; Beech et al. 2002; Engler et al. 2004). The

✉ Jin-Won Park
jwpark@seoultech.ac.kr

¹ Department of Chemical and Biological Engineering, Gachon University, Seongnam, Gyeonggi-do 461-701, South Korea

² Department of Chemical and Biomolecular Engineering, College of Energy and Biotechnology, Seoul National University of Science and Technology, 232 Gongneung-ro, Nowon-gu, Seoul 139-743, South Korea

forces on the approach of the AFM probe tip to the sample can be measured for electrostatic and steric effects, while the retraction of the force curves often shows a hysteresis for the adhesive properties. Many experimental force data are now available in the literature, and theoretical models have been developed for the analysis of forces acting between two solid surfaces and to a lesser extent the properties of thin films (Senden et al. 1994; Biggs 1995; van der Vegte and Hadziioannou 1997; Cappella and Dietler 1999; Dimitriadis et al. 2002). In this work, we aim to investigate the effect of trehalose on the mechanical properties of liposome, including the comparison to that of glucose.

Experiments

Dipalmitoylphosphatidylcholine (DPPC) and trehalose(α -D-glucopyranosyl- α -D-glucopyranoside) were purchased from Avanti Polar Lipids (Alabaster, AL) and Sigma Aldrich (St. Louis, MO), respectively. These reagents were used without further purification. The DPPC was dissolved in chloroform, subsequently under a dry stream of nitrogen to obtain the lipid film at the bottom of a glass tube. The film was overnight kept at low pressure to remove last traces of impurities of the organic solvent. To the films, 2 ml of a buffer containing 10 mM Hepes, 50 mM KCl, 1 mM NaN_3 , and trehalose at pH 7 was added. The amount of trehalose was determined with the desired ratio of trehalose to DPPC (0, 0.1, 0.3, 0.5, 0.7, and 1.0). While the lipid suspension was kept for at least 2 h above 10 °C above the gel–fluid transition temperature, the suspension was vortexed vigorously every 20 min four times. Large unilamellar vesicles were made by extruding the suspension through two stacked 100-nm pore size polycarbonate filters, and analyzed for diameter using dynamic light scattering (ELS-8000, Otsuka, Tokyo, Japan). The diameter was found to be approximately 150 ± 20 nm.

AFM experiments were performed at 25 °C using a liquid cell (Nanoscope v5.12, Veeco, Santa Barbara, CA). Mica peeled off was placed on the AFM scanner, and brought close to the cantilever tip mounted onto the cell. The cell-inside, sealed completely with a silicon O-ring, was fully filled with the vesicle solution. The solution covered a whole mica surface in the cell, and the vesicles adsorbed onto the surface at room temperature for 1 h. After non-adsorbed vesicles were removed by flushing the cell-inside with the buffer solution, the topographic images were taken in the constant-deflection mode. After the forces between the tip and the vesicle were measured on and around the vesicles, only the curves of the forces with two jump-in points and the highest onset point were selected and analyzed.

The force curves were analyzed with the Hertzian contact model (Laney et al. 1997; Radmacher et al. 1994). The model describes that the indentation from the difference between the cantilever position change $z - z_0$ and the cantilever deflection $d - d_0$ is given by the equation:

$$|z - z_0| - (d - d_0) = \delta = A(d - d_0)^{\frac{2}{3}} \\ = 0.825 \left[\frac{k^2(R_{\text{tip}} + R_{\text{ves}})(1 - \nu_{\text{ves}}^2)^2}{E_{\text{ves}}^2 R_{\text{tip}} R_{\text{ves}}} \right]^{\frac{1}{3}} (d - d_0)^{\frac{2}{3}}, \quad (1)$$

where δ is the indentation; A is a parameter; k is the cantilever spring constant; R_{tip} and R_{ves} are the radius of the tip and vesicle, respectively; ν_{ves} is the Poisson's ratio of the vesicle; and E_{ves} is the Young's modulus of the vesicle. In this model, there are two fit parameters, A and z_0 . The z_0 value was generally found to be consistent with the visually examined contact point and estimated by the onset point of the repulsive force. The A value was obtained by least square fitting. Only data with indentation less than 10 nm can be fitted to the equation to ensure elastic behavior (Laney et al. 1997). Then, E_{ves} was calculated from A , and used to deduce a bending modulus k_c based on the equation:

$$k_c = \frac{E_{\text{ves}} h^3}{12(1 - \nu_{\text{ves}}^2)}, \quad (2)$$

where h is the bilayer thickness.

Results and Discussion

In nanometer-scale morphology, no significant change was found with respect to the trehalose concentration. No change was predicted, because extrusion above the transition temperature of the lipids was performed in order to remove the effect of the change in the diameter on the mechanical properties. In this research, study was conducted only on the effect of the trehalose interference on the properties. The AFM images were shown in Fig. 1. The image prior to the vesicle solution injection is presented in Fig. 1a. In Fig. 1a, maximum step height is observed as less than 1 nm, and the cross-sectional width of most morphological bumps is found almost flat. Figure 1b shows the image after the vesicle adsorption and step height up to almost 10 nm and cross-sectional width of most bumps around 190 ± 60 nm.

The force curves provide stepwise mechanical deformation events on the vesicles. Figure 2a shows a deflection versus z position plot on vesicle made with the buffer solution of 0 % trehalose concentration. Figure 2b is a

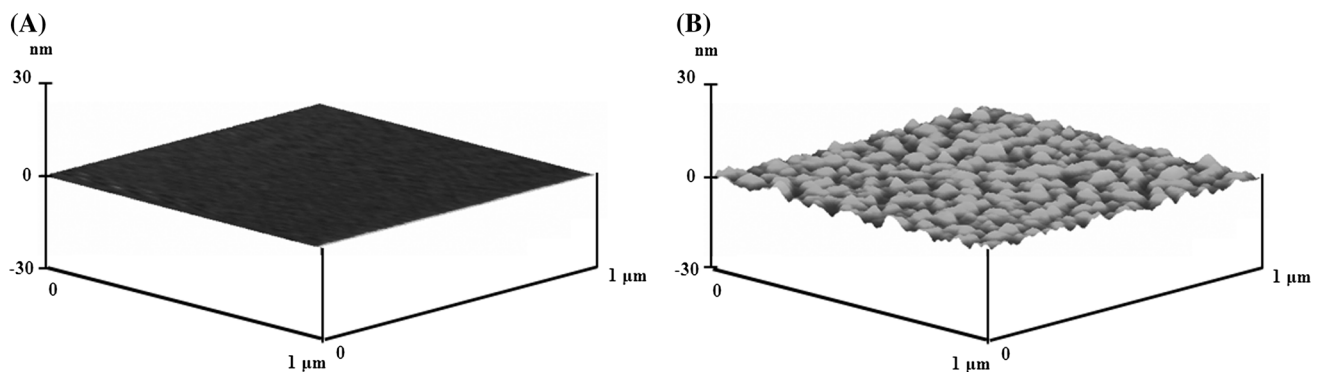


Fig. 1 AFM images **a** before the lipid vesicle adsorption, **b** after the lipid vesicle adsorption

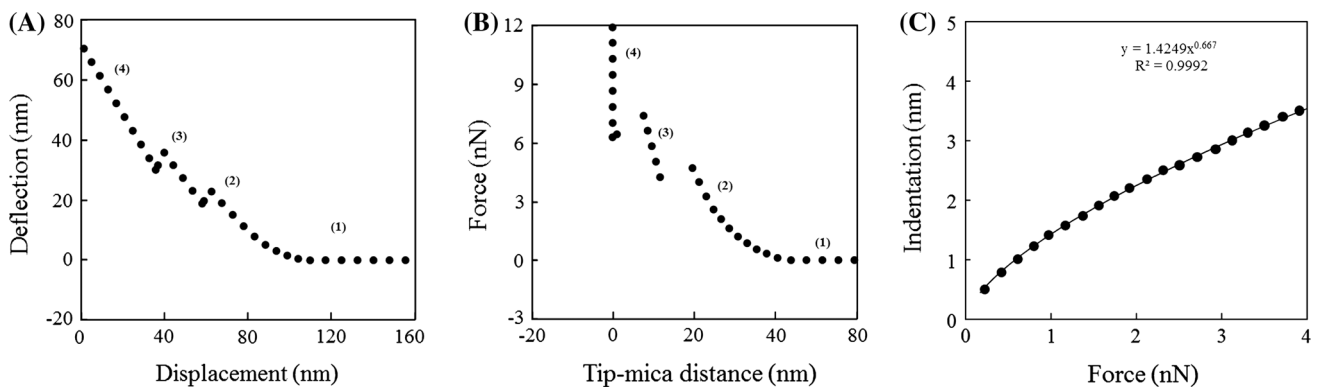


Fig. 2 **a** Deflection versus z position plot on DPPC vesicle at 0 % trehalose, **b** force versus distance plot based on the data from (a), **c** indentation versus load force plot based on the data from (a) region (2)

force with respect to the distance between the tip and a vesicle, which is based on the data from Fig. 2a. The curves in Fig. 2a, b can be divided into four regions as labeled. In region (1), the tip was far away from vesicle, and no deflection of the tip was observed. Region (2) illustrates the elastic deformation of the vesicle under tip compression and therefore can be used to calculate the Young's modulus. Region (3) corresponds to further tip compression after the tip penetrates the vesicle's top bilayer. In region (4), the cantilever penetrated the vesicle's bottom bilayer in contact with the hard mica substrate. Theoretically, the slope of region (4) should be around 1.0 because the deflection of the cantilever is identical to the z direction movement of sample on hard surface (Weisenhorn et al. 1993). From the fitting of the data, the slope was 0.995. The two jump-in points during the rise of the steric repulsion correspond to the tip penetrating the upper and lower portion of each vesicle, respectively (Liang et al. 2004). Onset of repulsive regime on the bilayer found at around 6 nm suggests that there was no bilayer adsorbed onto the tip, and the force measurements were conducted on mica. This suggestion is supported from comparison of force curves made with a clear tip in pure water and with the tip in the vesicle solution for several hours.

The slope of a force curve describes the elastic properties of a sample (Laney et al. 1997; Weisenhorn et al. 1993). The slope values of the first repulsive region (2) and second repulsive region (3) before and after the first breakthrough point for the molar ratio of trehalose to DPPC are listed separately in Table 1. The experimental results shown are average values, and the range of the results is less than 3 %. The values lay in the range of 0.64–0.69 and 3.3–3.5 N/m. By comparison, the slope values for the 0 % trehalose concentration of the two repulsive force regimes are 0.7 and 3.6 N/m, respectively. By fitting experimental data (region (2) and region (3)) to the Hertzian contact model $\delta = AF^b$ (where F is loading force), the exponent b was 0.667 (region (2)) and 0.905 (region (3)), respectively. The exponent b of the deflection is $2/3$ in the model, as shown Eq. (1). The poor fit on the region (3) indicates that the Hertzian model is not suitable for the region (3). Although the Hertzian model describes the contact between two solid bodies on the basis of continuum elasticity theory without adhesion force (Radmacher et al. 1994), the good fit in region (2) suggests that the Hertzian model may also be applicable to describe the elastic deformation between the tip and the vesicle within the limit of small indentation. Region (2) of Fig. 2a, b illustrated the elastic deformation

Table 1 Slope of the repulsive forces on the DPPC vesicles with respect to the ratio of trehalose to lipid

| Ratio of trehalose to lipid | 0 | 0.1 | 0.3 | 0.5 | 0.7 | 1.0 |
|------------------------------------|-----|------|------|------|------|------|
| Slope of 1st repulsive force (N/m) | 0.7 | 0.69 | 0.67 | 0.65 | 0.65 | 0.64 |
| Slope of 2nd repulsive force (N/m) | 3.6 | 3.5 | 3.4 | 3.3 | 3.3 | 3.3 |

of the vesicle under tip compression, thus all subsequent calculations for determining the nanomechanical properties of the vesicle surfaces were conducted to the data in region (2) based on the Hertzian model. Figure 2c is the indentation versus load force based on the data from Fig. 2a region (2). It presents that there is a good agreement between the experiment findings and the Hertzian model. The calculations with Eqs. (1) and (2) led to the estimations of the moduli with bilayer thickness (h) 5 nm. It should be noted that the value of Young's modulus is slightly affected by the value of Poisson's ratio (e.g., 10 % deviation of Poisson's ratio from 0.5 to 0.45 causes 6 % increase of Young's modulus). In contrast, the bending modulus would not be affected by Poisson's ratio variation.

Table 2 lists the Young's modulus and the bending modulus of DPPC vesicles with respect to the trehalose concentration calculated based on AFM approaching force curves. Compared with DPPC vesicles at 0 % trehalose, the moduli of the trehalose-incorporated vesicles were found to decrease obviously. The Young's modulus and the bending modulus of the DPPC vesicles without the incorporation were 81×10^6 Pa and 11.3×10^{-19} J, respectively, which were in good agreement with previous research (Lee et al. 2001). It is plausible that the elastic-property change is due to the trehalose. The incorporation of the trehalose seems to lead to the change in the headgroup packing geometrical structures. From the previous research, it has been proposed that the increase in the sugar:lipid ratio led to an increase in the lamellar repeat spacing caused by the incorporation (Lennéa et al. 2010). In the research, it was also found that above 0.5 disaccharide molecules per lipid,

the increase was not proportional with the sugar composition. These results are consistent with the change in the mechanical properties estimated in this research. It was suggested that the sugars induced the osmotic and volumetric effects on the membranes (Koster et al. 2000). Moreover, it has been shown that excess sugars were observed for disaccharide of solute:lipid ratios more than 0.5:1 and excluded from the hydration layer near phospholipid headgroups (Westh 2008).

Furthermore, interestingly, the effect of the trehalose on the properties was considerably different from that of glucose. Since the trehalose is a dimer of glucose, the same measurements were repeated at the glucose twice of the trehalose concentration. Only a slight decrease of the properties was observed at the glucose. The Young's modulus and the bending modulus were kept at even 2:1 ratio of glucose:lipid around 80×10^6 Pa and 11.3×10^{-19} J, respectively. All of the results described above seem attributable to the osmotic and volumetric effects on the headgroup packing disruption. The results were supported from the previous results that the ratio of the sugar to the lipid at which no exclusion occurred was in a specific range, independent of the lipid layer phase (Lambruschini et al. 2000). This interpretation seems to be supported by the molecular dynamic simulation in which the hydrogen bonding by the trehalose for the solid phase of the biological membranes promoted the order of the lipid tails (Pereira and Hünenberger 2006).

The previous investigations proposed that the trehalose enabled the membrane to be stabler for the liquid phase of the membranes, and were useful to understand the membrane phenomena for the thermal and mechanical stresses (Kapla et al. 2013, Kent et al. 2014, Brüning et al. 2014). The results from the present study with the solid phase of the lipid layers appear uniquely consistent with the hypothesis that the biological functions are preserved at lower than the lipid transition temperature. From the present and previous studies, it is inferred that the trehalose may induce the opposite phase for each other as cholesterol does.

Conclusion

In this study, the Young's modulus (E) and the bending modulus (k_c) for DPPC vesicles are estimated by analyzing AFM approach force curves based on the Hertzian model.

Table 2 Comparison of Young's modulus (E_{ves}) and bending modulus (k_c) values of the DPPC vesicles with respect to the ratio of trehalose/lipid and glucose/lipid

| | Ratio of trehalose/lipid | | | | | |
|-----------------------------------|--------------------------|------|------|------|------|------|
| | 0 | 0.1 | 0.3 | 0.5 | 0.7 | 1.0 |
| $E_{\text{ves}} \times 10^6$ (Pa) | 81 | 80 | 78 | 76 | 75 | 75 |
| $k_c \times 10^{-19}$ (J) | 11.3 | 11.2 | 10.8 | 10.5 | 10.4 | 10.4 |
| | Ratio of glucose/lipid | | | | | |
| | 0 | 0.2 | 0.6 | 1.0 | 1.4 | 2.0 |
| $E_{\text{ves}} \times 10^6$ (Pa) | 81 | 81 | 81 | 81 | 81 | 81 |
| $k_c \times 10^{-19}$ (J) | 11.3 | 11.3 | 11.3 | 11.3 | 11.3 | 11.3 |

The Young's modulus and the bending modulus decreased proportionally to the increase in the trehalose concentration up to 0.5 of trehalose to lipid. In the identical measurements for glucose, just a slight change in the modulus was observed with the increase in the glucose composition from 0 % glucose up to even 2:1 ratio of glucose:lipid. These results seem attributable to the osmotic and volumetric effects on the headgroup packing disruption. The present study may provide a platform to control biological functions related to cellular processes. Therefore, it would be interesting to investigate the saccharide effect on the behavior of the agent-triggered cells.

Acknowledgments This research was supported by the Basic Science Research Program through the National Research Foundation of Korea (NRF) funded by the Ministry of Education (2010-0010097). The authors thank all of the members of the Department of Chemical and Biomolecular Engineering at the Seoul National University of Science and Technology for help and valuable discussions. The authors also thank Prof. Heongkyu Ju and Mr. Jisu Kim at the Gachon University for their valuable help.

References

- Beech IB, Smith JR, Steele AA, Penegar I, Campbell SA (2002) The use of atomic force microscopy for studying interactions of bacterial biofilms with surfaces. *Colloids Surf B Biointerfaces* 23:231–247
- Biggs S (1995) Steric and bridging forces between surfaces bearing adsorbed polymer—an atomic-force microscopy study. *Langmuir* 11:156–162
- Brüning B-A, Prévost S, Stehle R, Steitz R, Falus P, Farago B, Hellweg T (2014) Bilayer undulation dynamics in unilamellar phospholipid vesicles: effect of temperature, cholesterol and trehalose. *Biochim Biophys Acta* 1838:2412–2419
- Cappella B, Dietler G (1999) Force-distance curves by atomic force microscopy. *Surf Sci Rep* 34:1–104
- Carpenter JF, Crowe LM, Crowe JH (1987) Stabilization of dry phospholipid bilayers and proteins by sugars. *Biochim Biophys Acta* 923:109–115
- Crowe JH, Crowe LM (1992) *Water and life*. Springer, Berlin
- Crowe LM, Crowe JH (1995) *Liposomes, new systems and new trends in their applications*. Editions de Santé, Paris
- Crowe JH, Crowe LM, Jackson SA (1983) Preservation of structural and functional activity in lyophilized sarcoplasmic reticulum. *Arch Biochem Biophys* 220:477–484
- Crowe LM, Crowe JH, Rudolph A, Womersley C, Appel L (1985) Preservation of freeze-dried liposomes by trehalose. *Arch Biochem Biophys* 242:240–247
- Dimitriadis EK, Horkay F, Maresca J, Kachar B, Chadwick RS (2002) Determination of elastic moduli of thin layers of soft material using the atomic force microscope. *Biophys J* 82:2798–2810
- Engler AJ, Richert L, Wong JY, Picart C, Discher DE (2004) Surface probe measurements of the elasticity of sectioned tissue, thin gels and polyelectrolyte multilayer films: correlations between substrate stiffness and cell adhesion. *Surf Sci* 570:142–154
- Fang HHP, Chan K-Y, Xu L-C (2000) Quantification of bacterial adhesion forces using atomic force microscopy (AFM). *J Microbiol Methods* 40:89–97
- Fendler JH (1982) *Biomimetic membranes*. Wiley, New York
- Kapla J, Wohler J, Svensson B, Engström Widmalm G, Maliniak A (2013) Molecular dynamics simulations of membrane–sugar interactions. *J Phys Chem B* 117:6667–6673
- Kent B, Hunt T, Darwich TA, Hauß T, Garvey CJ, Bryant G (2014) Localization of trehalose in partially hydrated DOPC bilayers: insights into cryoprotective mechanisms. *J R Soc Interface* 11:20140069
- Koster KL, Lei YP, Anderson M, Martin S, Bryant G (2000) Effects of vitrified and nonvitrified sugars on phosphatidylcholine fluid-to-gel phase transitions. *Biophys J* 78:1932–1946
- Lambruschini C, Relini A, Ridi A, Cordone L, Gliozzi A (2000) Trehalose interacts with phospholipid polar heads in Langmuir monolayers. *Langmuir* 16:5467–5470
- Laney DE, Garcia RA, Parsons SM, Hansma HG (1997) Changes in the elastic properties of cholinergic synaptic vesicles as measured by atomic force microscopy. *Biophys J* 72:806–813
- Lee C-H, Lin W-C, Wang JP (2001) All-optical measurements of the bending rigidity of lipid-vesicle membranes across structural phase transitions. *Phys Rev E* 64:020910(R)
- Lennéa T, Garvey CJ, Koster KL, Bryant G (2010) Kinetics of the lamellar gel–fluid transition in phosphatidylcholine membranes in the presence of sugars. *Chem Phys Lipids* 163:236–242
- Lerbret A, Bordat P, Affouard F, Hédoux A, Guinet Y, Descamps M (2007) How do trehalose, maltose, and sucrose influence some structural and dynamical properties of lysozyme? Insight from molecular dynamics simulations. *J Phys Chem B* 111:9410–9420
- Leslie SB, Teter SA, Crowe LM, Crowe JH (1994) Trehalose lowers membrane phase transitions in dry yeast cells. *Biochim Biophys Acta* 1192:7–13
- Liang X, Mao G, Ng KYS (2004) Probing small unilamellar EggPC vesicles on mica surface by atomic force microscopy. *Colloids Surf B Biointerfaces* 34:41–51
- Pereira C, Hünenberger PH (2006) Interaction of the sugars trehalose, maltose and glucose with a phospholipid bilayer: a comparative molecular dynamics study. *J Phys Chem B* 110:15572–15581
- Radmacher M, Fritz M, Kacher CM, Walters DA, Hansma PK (1994) Imaging adhesion forces and elasticity of lysozyme adsorbed on mica with the atomic-force microscope. *Langmuir* 10:3809–3814
- Senden TJ, Drummond CJ, Kékicheff P (1994) Atomic-force microscopy—imaging with electrical double-layer interactions. *Langmuir* 10:358–362
- Svetina S, Zeks B (1996) *Handbook of nonmedical applications of liposomes*. CRC Press, Boca Raton
- van der Vegte EW, Hadzioannou G (1997) Scanning force microscopy with chemical specificity: an extensive study of chemically specific tip–surface interactions and the chemical imaging of surface functional groups. *Langmuir* 13:4357–4368
- Weisenhorn AL, Khorsandi M, Kasas S, Gotz S, Butt H-J (1993) Deformation and height anomaly of soft surfaces studied with an AFM. *Nanotechnology* 4:106–113
- Westh P (2008) Glucose, sucrose and trehalose are partially excluded from the interface of hydrated DMPC bilayers. *Phys Chem Chem Phys* 10:4110–4112